Optical-Model Analysis of p-O^{16} Elastic Scattering from 23–53 MeV

W. T. H. VAN OERS*
Department of Physics, University of Manitoba, Winnipeg, Canada
AND
J. M. CAMERON†
Department of Physics, University of California, Los Angeles, California

(Received 5 February 1969)

Differential cross section and polarization angular distributions for p-O^{16} elastic scattering together with total-reaction cross section data in the energy range 23–53 MeV were analyzed using the eleven-parameter optical-model search code SEEK. The optical potential contains a surface-absorption term of Gaussian form rather than the usual Woods-Saxon derivative form. Emphasis was placed upon finding the energy dependence of the strengths of the potentials. Consequently, an averaged set of geometrical parameters was first defined, and then a search was made for the strengths of the real central, the volume and surface parts of the imaginary central, and the real spin-orbit potentials. The energy dependence of the real central potential for O^{16} in the energy range 23–53 MeV can be represented by $dV/dE \cong -0.29$. The fits to the large-angle data are in general unsatisfactory. Difficulties were encountered in fitting the three sets of data below 30 MeV. This is consistent with what is expected from the nonmonotonic energy behavior of the differential cross sections and polarizations in this energy region.

I. INTRODUCTION

THE nuclear optical-model potential is in general energy-dependent and nonlocal. The energy dependence of the real and imaginary parts of the optical-model potential can be represented by a dispersion relation.[1,2] The phenomenological optical-model potentials whose parameters are obtained by fitting elastic scattering data are usually chosen to be local potentials. Because of the nonlocality of the general optical-model potential, the equivalent phenomenological local potential will contain a spurious energy dependence in addition to the intrinsic or dynamical energy dependence. Studies of the energy dependence of phenomenological optical-model potentials have been undertaken by Passatore,[3] and Lipperheide and Schmidt.[4] These studies are hampered by a lack of systematic optical-model analyses of the elastic scattering from a given nucleus over a large energy range. Of course, a prerequisite for such analyses is the availability of accurate elastic scattering data over a wide range of energies. In this sense the present analysis of $p+O^{16}$ elastic scattering in the rather limited energy range 23–53 MeV should be considered as a first attempt only. An extension of the analysis must wait until experimental data in the 50–200 MeV range become available. To determine the energy dependence of the phenomenological optical-model potential one generally determines first an averaged set of geometrical parameters, i.e., the average radius and diffuseness parameters. The energy dependence is then exhibited by the behavior of the dynamical parameters, i.e., the strengths of the various potential terms, as a function of energy.

The strength of the real part of the central potential shows a well marked general decrease with energy. This can be understood qualitatively as a result of averaging over the nucleon-nucleon potentials. The average contains overlap integrals between the wave functions of the incident particle and the target nucleus, and thus decreases with energy. The repulsive core in the nucleon-nucleon interaction becomes more important at higher energies, and this also causes a decrease in the average potential.

The energy dependence of the strength of the real part of the central potential has been investigated by several authors. Buck[5] analyzed proton elastic and inelastic scattering data in the energy region 10–20 MeV for medium mass nuclei using a generalized optical model and deduced the energy dependence

$$V = 52.6 \text{ MeV} - 0.28E \pm 1.0 \text{ MeV}.$$

Perey[6] found it necessary to add an extra term to take account of the decrease in the kinetic energy of the proton inside the nucleus caused by the Coulomb potential. Perey's analysis resulted in,

$$V = 53.3 \text{ MeV} - 0.55E + [0.4(Z/A^{1/3}) + 27(N-Z)/A] \text{ MeV},$$

where Z and A have the usual meaning. A more recent analysis of proton elastic scattering data by Rosen *et al.*,[7] again in the energy range 10–20 MeV, yielded

* Supported in part by the Atomic Energy Control Board of Canada.
† Supported in part by the U.S. Atomic Energy Commission, Present address: Department of Physics, University of Washington, Seattle, Wash.

[1] H. Feshbach, Ann. Phys. (N.Y.) **5**, 357 (1958).
[2] J. M. Cornwall and M. A. Ruderman, Phys. Rev. **128**, 1474 (1962).
[3] G. Passatore, Nucl. Phys. **A110**, 91 (1968).
[4] R. Lipperheide and A. K. Schmidt, Nucl. Phys. **A112**, 65 (1968).
[5] B. Buck, Phys. Rev. **130**, 712 (1963).
[6] F. G. Perey, Phys. Rev. **131**, 745 (1963).
[7] L. Rosen, J. G. Beery, A. S. Goldhaber, and E. H. Auerbach, Ann. Phys. (N.Y.) **34**, 96 (1965).

for the energy dependence

$$V=53.8\text{ MeV}-0.33E.$$

The energy dependence in the region 30–40 MeV has been determined by Fricke *et al.*[8] Their analysis resulted in

$$V=49.9\text{ MeV}-0.22E+[0.4(Z/A^{1/3})+26.4(N-Z)/A]\text{ MeV}.$$

This relation is quite different from that at the lower energies, and thus a further investigation of this relationship at energies between 20 and 50 MeV would appear to be desirable.

Phenomenological results for the imaginary part of the central potential show an increase in the depth from about 3 MeV at low-incident energies to about 20 MeV at an energy of 100 MeV where it flattens out. The increase may be understood qualitatively as a consequence of the Pauli exclusion principle, which forbids collisions which would promote particles to states which are already occupied. Because all states of low energy are filled, the exclusion principle is more restrictive at low energies, resulting in less absorption and in a surface peaked form factor for the absorption potential. The absorption potential has been stated to be in general a mixture of surface and volume terms. At lower energies, elastic scattering is insensitive to the ratio of surface to volume absorption although there is a general preference for a predominant surface form. There are indications[6] that a small volume component improves the fit to 22-MeV proton-scattering data. The analysis of 30-MeV data[9] and of 40 MeV data[8] indicates that a small volume absorption of 2–4 MeV is required to fit these data. Finally, the analysis[10] of 180-MeV data showed that for these energies the absorption is all volume.

The present analysis has been undertaken to determine the energy dependence of the dynamical optical-model parameters for $p+O^{16}$ elastic scattering between 23 and 53 MeV. A similar analysis was performed recently by Gross *et al.*[11] for $p+Ca^{40}$ elastic scattering in the energy range 30–45 MeV. With fixed geometrical parameters the latter analysis resulted in an energy dependence of the real central well of $dV/dE=-0.32$, while the strengths of the surface and volume terms of the imaginary central well showed a relatively smooth decrease and increase, respectively, with increasing incident proton energy. For the $p+O^{16}$ optical-model analysis data at twelve different energies were selected. The data selection is presented in Table I. The elastic-scattering angular distributions show a smooth variation with energy for incident proton energies above 30 MeV. Below 30 MeV, however, the angular distributions exhibit strong variations with energy, especially at the backward angles. A subsequent more detailed investigation[12] of this energy dependence revealed the existence of peaks in excitation functions at a number of backward angles. The elastic scattering excitation functions for the energy range 20–30 MeV integrated over the backward hemisphere showed resonances several hundred keV wide. The nonmonotonic behavior with energy has been attributed to resonances in the compound system F^{17}. This is analogous to the situation encountered between 20 and 30 MeV in $p-C^{12}$ elastic scattering. In that case the irregular variation with energy of the differential cross section and polarization angular distributions could be explained[13] fairly successfully by adding to the optical-model potential scattering amplitude Breit-Wigner terms corresponding to resonances in the compound system N^{13}. In view of the nonmonotonic variation with energy of the $p+O^{16}$ angular distributions below 30 MeV, difficulties

TABLE I. Data selection for the $p+O^{16}$ optical-model analysis in the energy range 23–53 MeV.

E (MeV)	$\sigma(\theta)$ (Reference)	$P(\theta)$ (Reference)	σ^r (Reference)
23.4	a	b	
24.5	a	b	
27.3	a	c	d
30.1	a	c	d
34.1	a	c	d
36.8	a	c	
39.7	a	c	d
42.1	b	b	
43.1	a		d
46.1	a		d
49.5	e		
52.5	b	b	

[a] J. M. Cameron, J. R. Richardson, W. T. H. van Oers, and J. W. Verba, Phys. Rev. **167**, 908 (1968).

[b] E. T. Boschitz, M. Chabre, H. E. Conzett, and R. J. Slobodrian, in *Proceedings of the Second International Symposium on the Polarization Phenomena of Nucleons*, edited by P. Huber and H. Schopper (Birkhäuser Verlag, Stuttgart, Germany, 1966), p. 331.

[c] H. B. Eldridge, S. N. Bunker, J. M. Cameron, J. R. Richardson, and W. T. H. van Oers, Phys. Rev. **167**, 915 (1968).

[d] R. F. Carlson, J. M. Cameron, W. F. McGill, J. R. Richardson, and J. W. Verba, Bull. Am. Phys. Soc. **16**, 1190 (1967).

[e] J. A. Fannon, E. J. Burge, D. A. Smith, and N. K. Ganguly, Nucl. Phys. **A97**, 263 (1967).

[8] M. P. Fricke, E. E. Gross, B. J. Morton, and A. Zucker, Phys. Rev. **156**, 1207 (1967).

[9] G. R. Satchler, Nucl. Phys. **A92**, 273 (1967).

[10] R. M. Haybron and G. R. Satchler, Phys. Letters **11**, 313 (1964).

[11] E. E. Gross, R. H. Bassel, L. N. Blumberg, B. J. Morton, A. van der Woude, and A. Zucker, Nucl. Phys. **A102**, 673 (1967).

[12] H. Appel, S. N. Bunker, J. M. Cameron, M. B. Epstein, J. R. Quinn, J. R. Richardson, and J. W. Verba, Bull. Am. Phys. Soc. **13**, 680 (1968).

[13] J. Lowe and D. L. Watson, Phys. Letters **23**, 261 (1966); **24B**, 174 (1967).

can be expected for the optical-model analysis in that energy region, in particular in reproducing the backward parts of the experimental angular distributions. Between 10 and 20 MeV, the analysis of $p+O^{16}$ differential cross sections by Duke[14] showed that satisfactory fits to the data could only be obtained by varying the strength of the surface absorptive potential and its diffuseness parameter rapidly with energy. Quite generally one expects the optical-model fits for a light nucleus such as O^{16} to be of poorer quality than those for average medium weight and heavy nuclei.

II. ANALYSIS

The optical-model analysis was performed using a local potential of the form

$$U(r)=V_c(r)-V[1/\{1+\exp(x_1)\}]$$
$$-iW[1/\{1+\exp(x_2)\}]$$
$$-iW_1\exp(-x_3^2)+(V_s+iW_s)(4/r)(d/dr)$$
$$\times[1/\{1+\exp(x_4)\}](\mathbf{s}\cdot\mathbf{l}).$$

In this expression $V_c(r)$ is the Coulomb potential for a uniformly charged sphere of radius $1.25A^{1/3}$F. The quantity V denotes the strength of the real central potential, while W and W_1 are the strengths of the volume and surface parts, respectively, of the imaginary central potential. The quantities V_s and W_s are the strengths of the real and imaginary parts of the spin-orbit potential. The shape factors for the real central and the volume part of the imaginary central potential are of the Woods-Saxon form. The surface part of the imaginary central potential has a Gaussian form while the shape factor for the spin-orbit potential is of the usual Thomas type. The remaining factors in the exponential functions contain the radius and diffuseness parameters. They are defined as follows:

$$x_1=(r-R)/a, \qquad x_2=(r-R_i)/a_i,$$
$$x_3=(r-R_i)/b_i, \qquad x_4=(r-R_s)/a_s,$$
$$R=r_0A^{1/3}, \qquad R_i=r_iA^{1/3},$$

and

$$R_s=r_sA^{1/3}.$$

To reduce the number of free parameters, the relationship $a_i=0.69b_i$ was introduced which makes both volume and surface absorptions drop to one-tenth of their maximum value at the same radius.

The $p+O^{16}$ differential cross section and polarization data were analyzed using an eleven-parameter automatic search code. This code is a modified version of the program SEEK[15] which allows the spin-orbit geometrical parameters to be varied independently. The calculations were done fitting simultaneously to the differential cross section and polarization data by minimization of the quantity χ^2. Here, χ^2 was defined as

$$\chi^2=\chi^2_\sigma+\chi^2_P$$

where

$$\chi^2_\sigma=\sum_{j=1}^{N_\sigma}\left[\frac{\sigma_{\text{theor}}(\theta_j)-\sigma_{\text{expt}}(\theta_j)}{\Delta\sigma(\theta_j)}\right]^2,$$

and

$$\chi^2_P=\sum_{k=1}^{N_P}\left[\frac{P_{\text{theor}}(\theta_k)-P_{\text{expt}}(\theta_k)}{\Delta P(\theta_k)}\right]^2.$$

The summations extend over the number of experimental differential cross sections and polarizations, N_σ and N_P, respectively. The quantities $\sigma_{\text{theor}}(\theta_j)$ and $P_{\text{theor}}(\theta_k)$ are the theoretically obtained differential cross sections and polarizations while $\sigma_{\text{expt}}(\theta_j)$ and $P_{\text{expt}}(\theta_k)$ are the experimental values and $\Delta\sigma(\theta_j)$ and $\Delta P(\theta_k)$ are the experimental errors at each angle θ_j and θ_k, respectively.

If the optimum set of parameters gave a theoretical value of the reaction cross section $\sigma^r{}_{\text{theor}}$ which differed from the experimental value by more than the experimental error, then the program performed a sequence of constrained searches using a redefined χ^2, viz.,

$$\chi^2=\chi^2_\sigma+\chi^2_P+\chi^2_r,$$

where

$$\chi^2_r=[\sigma^r{}_{\text{theor}}-\bar{\sigma}^r)/\Delta\sigma^r]^2,$$

and

$$\bar{\sigma}^r=\bar{\sigma}^r{}_{\text{theor}}\pm\delta\sigma^r, \qquad \Delta\sigma^r=\delta^r\bar{\sigma}^r,$$

$\bar{\sigma}^r{}_{\text{theor}}$ being the value at the minimum χ^2 of the previous search and $\delta\sigma^r$ and δ^r being input quantities. This sequence of searches was continued until the whole range of experimental uncertainty between $\sigma^r{}_{\text{expt}}+\Delta_+\sigma^r{}_{\text{expt}}$ and $\sigma^r{}_{\text{expt}}-\Delta_-\sigma^r{}_{\text{expt}}$ was covered. The quantity $\Delta\sigma^r$ is an artificial error and was chosen much smaller than $\Delta_\pm\sigma^r{}_{\text{expt}}$ in order to insure that $\sigma^r{}_{\text{theor}}$ became very close to $\bar{\sigma}^r$ at the minimum χ^2.

Since the primary interest of the analysis was to investigate the energy dependence of the dynamical parameters (V, W, W_1, V_s, and W_s), an acceptable averaged set of geometrical parameters had first to be determined. There exist for the energy region of 30–50 MeV and for target nuclei with $A\geq 28$ various sets of averaged geometrical parameters.[8,16] However, it is not at all certain that these sets can be used for a nucleus as light as O^{16}. Therefore, the following procedure was adopted: Selecting Becchetti and Greenless's set of averaged parameters,[16] because they appeared most consistent with the O^{16} data, a search was made for V, W, and W_1. The values for V, W, and W_1 thus found were reentered into the program and a nine- or seven-parameter search was made depending on whether or not polarization data were available. The strength of

[14] C. B. Duke, Phys. Rev. **129**, 681 (1963).
[15] M. A. Melkanoff, J. Raynal, and T. Sawada, University of California at Los Angeles, Report No. 66-10 (unpublished).
[16] F. D. Becchetti and G. W. Greenless, J. H. Williams Laboratory of Nuclear physics, University of Minnesota Annual Report, 1967 (unpublished).

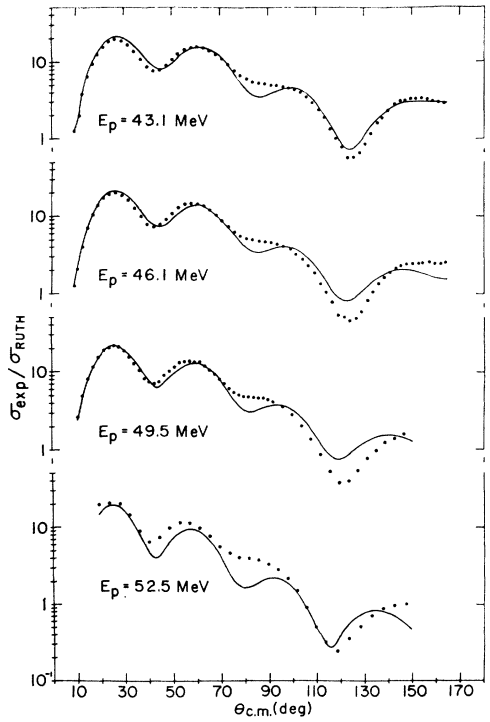

FIG. 1. The differential scattering cross sections divided by the Rutherford cross section for the elastic scattering of protons from O^{16} at 52.5, 49.5, 46.1, and 43.1 MeV. The 52.5-MeV data are of Table I, footnote b, the 49.5-MeV data are of Table I, footnote e, and the 46.1- and 43.1-MeV data are of Table I, footnote a. The solid lines represent the optical-model fits with fixed geometry.

the real spin-orbit potential was kept fixed (V_s= 6.20 MeV), while the imaginary spin-orbit potential (W_s) was set equal to zero. Later it was found that a search for W_s gave a very small value which did not improve the fits appreciably. Only the nine data sets with incident proton energies above 30 MeV were used to determine a new averaged set of geometrical parameters. The whole process was repeated resulting in an intermediate set of geometrical parameters. Next, with this intermediate set of geometrical parameters a search was made for V, W, W_1, and V_s. The values for V, W, W_1, and V_s thus found were re-entered into the program and a search was made once more for the geometrical parameters only. The resulting geometrical parameters were re-entered into the program and again a series of ten or seven parameter fits was made. Finally, the geometrical parameters for the best fits were averaged and fixed at the following values:

$$r_0=1.142\text{ F}, \quad r_i=1.268\text{ F}, \quad r_s=1.114\text{ F},$$
$$a=0.726\text{ F}, \quad a_i=0.676\text{ F}, \quad a_s=0.585\text{ F}.$$

This averaged geometry does not differ vastly from the averaged geometries for the same energy range[8,16] mentioned before. The only difference of importance is in the spin-orbit geometry for which the radius parameter obtained for O^{16} is only slightly smaller than the real central radius and for which the diffuseness is rather small.

With the geometry fixed, only four adjustable parameters were left, i.e., the four dynamical parameters V, W, W_1, and V_s. All 12 data sets were then fitted with the fixed geometry given above. An additional constraint required the calculated and experimental reaction cross sections to agree within the experimental error limits. In some cases visual examination of the fits served as a further guide. The fits to the 12 differential cross section angular distributions are shown in Figs. 1–3. It is apparent that for decreasing energy the quality of the fits deteriorates rapidly. Furthermore, the calculated angular distributions consistently show, for energies above 30 MeV, a pronounced minimum around 90° which is not observed experimentally. The fits to the nine polarization angular distributions are shown in Figs. 4 and 5. There is only qualitative agreement with the experimental angular distributions. Substantially improved fits could be obtained solely at the expense of reasonable differential cross section angular distribution fits. The strengths of the various potentials determined as described above are given in Table II. To compare the values for χ^2_σ

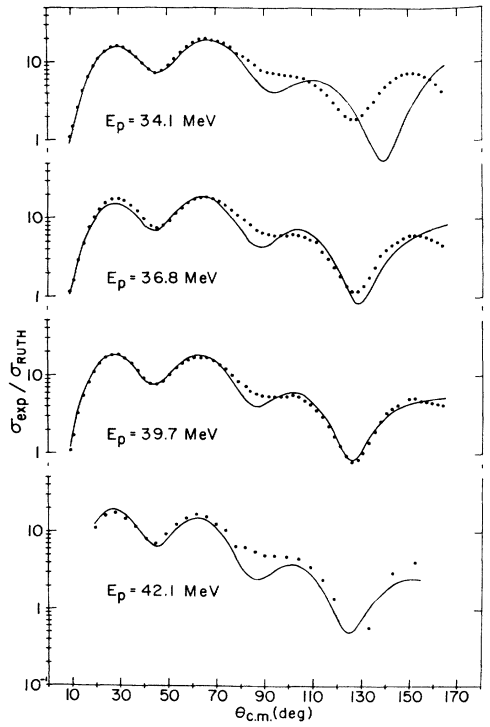

FIG. 2. The differential scattering cross sections divided by the Rutherford cross section for the elastic scattering of protons from O^{16} at 42.1, 39.7, 36.8, and 34.1 MeV. The 42.1 MeV data are of Table I, footnote b, and the 39.7, 36.8, and 34.1 MeV data are of Table I, footnote a. The solid lines represent the optical-model fits with fixed geometry.

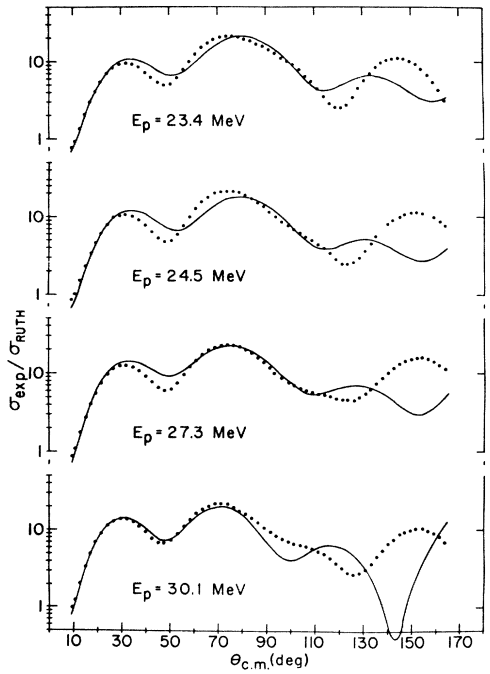

FIG. 3. The differential scattering cross sections divided by the Rutherford cross section for the elastic scattering of protons from O^{16} at 30.1, 27.3, 24.5, and 23.4 MeV. The data are of Table I, footnote a. The solid lines represent the optical-model fits with fixed geometry.

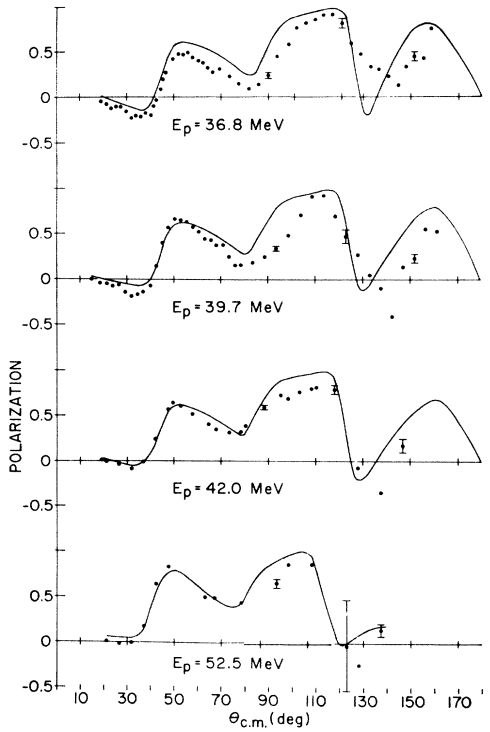

FIG. 4. Polarizations for the elastic scattering of protons from O^{16} at 52.5, 42.0, 39.7, and 36.8 MeV. Typical errors are indicated by the error bars. The 52.5 and 42.0 MeV data are of Table I, footnote b, and the 39.7 and 36.8 MeV data are of Table I, footnote c. The solid lines represent the optical-model fits with fixed geometry.

TABLE II. Optical-model potential strengths (in MeV) for the elastic scattering of protons from O^{16}. The potential strengths in parenthesis were kept fixed in the search. Also included in the table are the number of data points and the mean squares of the relative errors for each data set. The last two columns give the theoretical and experimental reaction cross sections in F^2. Square brackets in the last column indicate that the value for the reaction cross section was derived by interpolation.

E	V	W	W_1	V_s	W_s	χ^2_σ/N_σ	N_σ	$10^4((\Delta\sigma_{expt}/\sigma_{expt})^2)_{av}$	χ^2_P/N_P	N_P	$10^4((\Delta P_{expt}/P_{expt})^2)_{av}$	σ^r_{theor}	σ^r_{expt}
52.5	36.85	5.49	3.63	−4.93	(0.0)	9.18	31	100	11.7	15	35614	40.5	[40.0]
49.5	38.90	4.14	3.94	(−6.20)	(0.0)	82.3	54	7.82				39.0	[42.0]
46.1	42.13	4.44	4.64	(−6.20)	(0.0)	193.5	64	5.58				43.4	44.0
43.1	44.67	3.15	6.32	(−6.20)	(0.0)	180.0	64	1.72				46.2	46.7
42.1	43.10	2.83	6.25	−5.58	(0.0)	8.23	27	100	19.3	25	1517	45.3	[46.7]
39.7	46.58	2.25	7.65	−7.32	(0.0)	157.0	63	1.30	123.5	42	1547	49.0	46.6
36.8	46.37	0.28	8.55	−7.98	(0.0)	366.1	64	1.34	42.8	54	197.1	47.4	[48.5]
34.1	47.02	2.31	6.52	−6.44	(0.0)	1160	64	1.32	114.1	41	178.4	48.9	49.7
30.1	47.50	0.0	8.35	−6.82	(0.0)	1803	64	1.12	195.3	39	151.1	49.6	49.5
27.3	48.43	(0.0)	7.28	−5.63	(0.0)	1305	64	1.16	397.7	41	689.7	48.2	48.7
24.5	44.51	(0.0)	6.83	−5.41	(0.0)	1407	62	1.36	159.8	23	60.3	47.8	[48.5]
23.4	47.25	(0.0)	7.06	−4.09	(0.0)	923.1	64	1.33	53.6	25	202.0	49.9	[48.5]

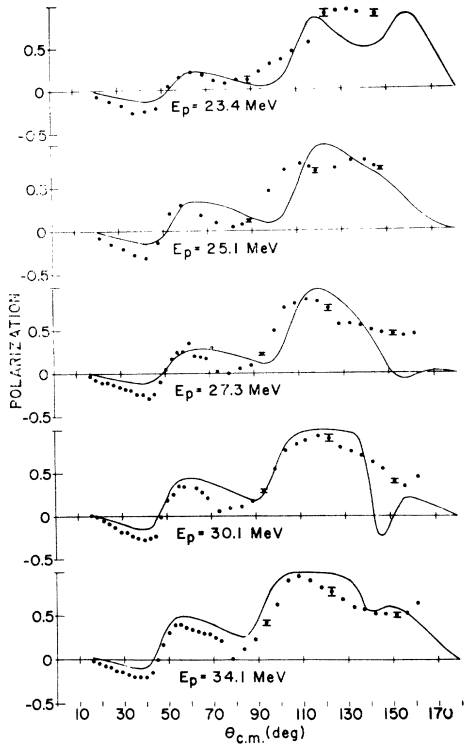

FIG. 5. Polarizations for the elastic scattering of protons from O^{16} at 34.1, 30.1, 27.3, 25.1, and 23.4 MeV. Typical errors are indicated by the error bars. The 34.1, 30.1, and 27.3 MeV data are of Table I, footnote c, and the 25.1 and 23.4 MeV data are of Table I, footnote b. The solid lines represent the optical-model fits with fixed geometry.

and χ^2_P in a relative manner these values are given together with the number of data points and with the mean square of the relative errors for each data set. The last two columns give the theoretical and experimental reaction cross sections, respectively. Square brackets in the last column indicate that the value for the reaction cross section was derived by interpolation. Variables in parentheses were kept fixed during the search.

III. DISCUSSION

Certain conclusions can be drawn from the parameters representing the averaged geometry. First it appears that the radius parameters satisfy the relation $r_s<r_0<r_i$. The differences are, however, less pronounced than those established for the averaged geometries for proton elastic scattering from a series of target nuclei with $A>28$ (Ref. 8) and $A\geq 40$ (Ref. 16). Furthermore, it is apparent that surface as well as volume absorption is needed for incident proton energies larger than 30 MeV.

The strengths of the central potentials (V, W, and W_1) obtained in the present analysis are shown in Fig. 6 together with the results of Duke[14] in the 8–20 MeV range and of Snelgrove and Kashy.[17] Assuming a linear energy dependence for the strength of the real central potential a slope $dV/dE\simeq -0.29$ is found for the energy range above 20 MeV. This value is intermediate to the values for dV/dE, obtained by Fricke *et al.*[8] as the average for ten different target nuclei in the energy region 30–40 MeV and by Gross *et al.*[11] for Ca^{40} in the energy region 30–45 MeV, viz,. $dV/dE=-0.22$ and -0.32, respectively. The solid line in Fig. 6 represents the least-squares, straight line fit to the values of the real central potential for the energy region above 20 MeV. Above 30 MeV the volume part of the imaginary central potential increases while the surface part decreases smoothly with increasing incident proton energy. In Fig. 6 the strength (W_1) of the surface absorption term has been multiplied by the width (b_i) of the surface absorption term to compare the results of the present analysis with those of Duke.[14] It was shown[14] that if the optical-model wave function is approximately constant over the nuclear surface, for a narrow Gaussian surface absorption, the reaction

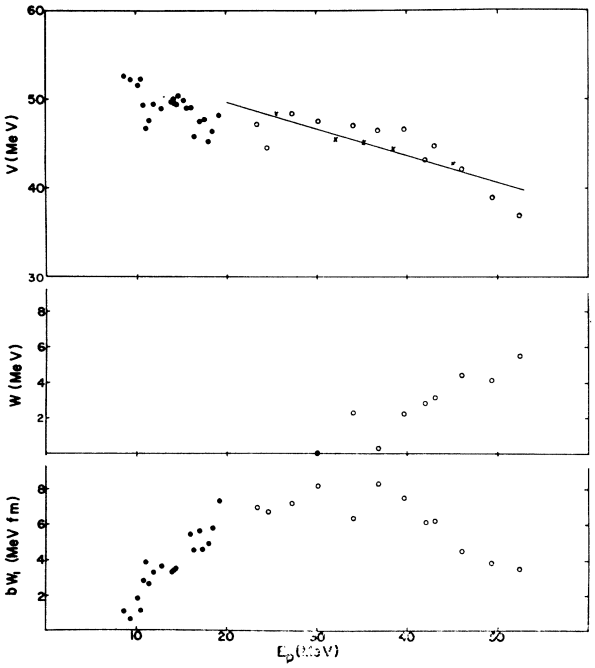

FIG. 6. Variation of the $p+O^{16}$ optical-model, central-well strengths (open circles) with incident proton energy for the fixed geometry given in the text. Also included in the figure are the results of optical-model analyses by Duke (Ref. 14, solid dots) and Snelgrove and Kashy (Ref. 17, crosses) of differential cross section angular distributions. The solid line represents a least-squares, straight line fit to the values for the strength of the real central potential in the energy range 20–50 MeV. The strengths of the surface imaginary central potential have been multiplied by the width of the surface potential.

[17] J. L. Snelgrove and E. Kashy, Bull. Am. Phys. Soc. **13**, 115 (1968); J. L. Snelgrove, Ph.D. thesis, Michigan State University, 1968 (unpublished).

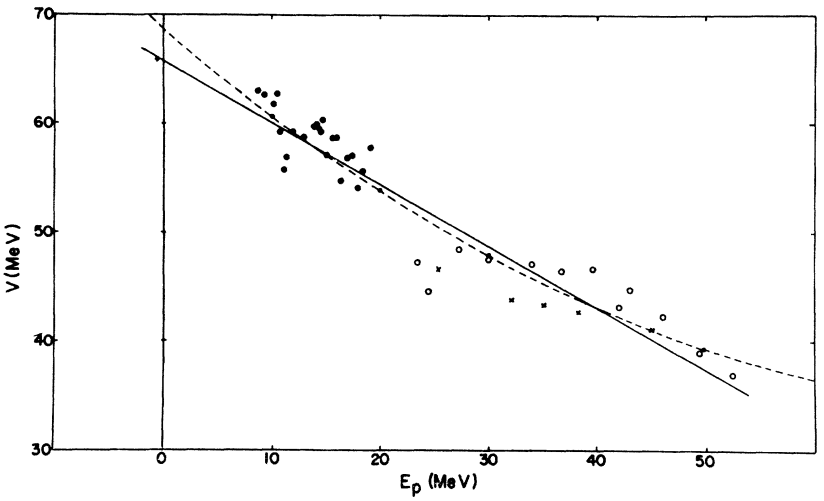

FIG. 7. Variation of the $p+O^{16}$ optical model, real central potential strengths with incident proton energy. All potential strengths were adjusted according to the Vr_0^2 law with $r_0=1.142$ F. The point at a negative proton energy was derived from the potential parameters for the ground state of F^{17} (Ref. 18). The solid and dashed lines represent least squares fits to the potential well strengths assuming a linear and a quadratic energy dependence, respectively.

cross section is proportional to the product $b_i \cdot W_1$. The strengths of the real part of the spin-orbit potential average out to a value of -6.02 MeV, which is very close to the value assumed in the searches at those energies for which polarization data were not available.

It is well known that optical-model analyses of proton elastic scattering data contain a Vr^2 ambiguity for the real central potential. As a check of this ambiguity a search was made for the dynamical parameters which gave fits to the 23.4, 24.5, and 27.3 MeV data with a geometry that differed from the best averaged geometry defined above only in the radius parameter for the real central potential ($r_0'=1.25$ F). It was found that the strengths of the real central potential were reduced to values very close to the predicted ones assuming a Vr^2 invariance, i.e., $(r_0/r_0')^2$ times the values given in Table II. To extract the energy dependence of the strength of the real central potential in the energy range 0–50 MeV, one should use parameters which are obtained in optical-model analyses with the same geometry. With the potential strengths adjusted according to the Vr^2 law, fixing the radius parameter r_0 at a value of 1.142 F, a linear energy dependence gives a slope $dV/dE \simeq -0.56$. The solid line in Fig. 7 represents the least-squares fit to the strengths of the real central potential in the energy range 0–50 MeV assuming a linear energy dependence. The point at a negative proton energy was derived from the potential parameters for the ground state of F^{17} as calculated by Tombrello.[18] It appears that the potential strengths have a slight preference for a quadratic energy dependence. The dashed line in Fig. 7 represents the least-squares fit to the strengths of the real central potential assuming a quadratic energy dependence. Accordingly, the energy dependence in the energy range 0–50 MeV can be represented by

$$V=68.76 \text{ MeV} -0.851E+0.00524E^2.$$

Obviously, this treatment of the real central potential strengths gives results which are not very satisfactory. It proves that the energy dependence of the dynamical parameters can only be determined in a reliable manner if all the experimental data are analyzed consistently, i.e., with the same form for the phenomenological optical-model potential and a common geometry.

In conclusion, the optical-model gives a fair description of the elastic scattering of protons from O^{16} for incident energies above 30 MeV, although the fits at backward angles are not altogether satisfactory. The nonmonotonic variation of the differential cross section and polarization angular distributions in the energy range 20–30 MeV is reflected in a similar nonmonotonic variation of the optical-model potential strengths with energy.

ACKNOWLEDGMENTS

The calculations were performed using the computing facilities of the UCLA Campus Computing Network and the University of Manitoba Institute for Computer Studies.

[18] T. A. Tombrello, Phys. Letters **23**, 134 (1966).